Molecular Nutrition & Food Research
www.mnf-journal.com

Postbiotics Prepared Using *Lactobacillus reuteri* Ameliorates Ethanol-Induced Liver Injury by Regulating the FXR/SHP/SREBP-1c Axis

Chen Liu, Tianying Cai, Yonglang Cheng, Junjie Bai, Mo Li, Boyuan Gu, Meizhou Huang, and Wenguang Fu**

Scope: While probiotics-based therapies have exhibited potential in alleviating alcohol-associated liver disease (ALD), the specific role of postbiotics derived from *Lactobacillus reuteri* (*L. reuteri*) in ALD remains elusive. This study aims to investigate the impact of postbiotics on ameliorating alcohol-induced hepatic steatosis and the underlying mechanisms.

Methods and results: Using network pharmacology, the study elucidates the targets and pathways impacted by postbiotics from *L. reuteri*, identifying the farnesoid X receptor (FXR) as a promising target for postbiotics against ALD, and lipid metabolism and alcoholism act as crucial pathways associated with postbiotics-targeting ALD. Furthermore, the study conducts histological and biochemical analyses coupled with LC/MS to evaluate the protective effects and mechanisms of postbiotics against ALD. Postbiotics may modulate bile acid metabolism in vivo by regulating FXR signaling, activating the FXR/FGF15 pathway, and influencing the enterohepatic circulation of bile acids (BAs). Subsequently, postbiotics regulate hepatic FXR activated by BAs and modulate the expression of FXR-mediated protein, including short regulatory partner (SHP) and sterol regulatory element binding protein-1c (SREBP-1c), thereby ameliorating hepatic steatosis in mice with ALD.

Conclusion: Postbiotics effectively alleviate ethanol-induced hepatic steatosis by regulating the FXR/SHP/SREBP-1c axis, as rigorously validated in both in vivo and in vitro.

1. Introduction

Alcohol-associated liver disease (ALD) arises from chronic alcohol consumption and is a significant health concern, leading to liver damage and progressing from hepatic steatosis to carcinoma, presenting distinct pathological features. Hepatic steatosis is the most common response of the liver to alcohol, with over 90% of heavy drinkers developing this reversible early stage of ALD.[1,2] Chronic alcohol intake contributes to gut barrier dysfunction, increased intestinal permeability, and alterations in intestinal homeostasis, all of which are factors contributing to the development of ALD through the gut-liver axis.[3] Currently, there are no accepted therapeutics to halt or reverse ALD in patients, despite the profound economic and health impact of ALD, and early prevention and treatment can efficiently attenuate the development of irreversible lesions.[4,5] Therefore, there is an urgent need to develop novel ALD therapies.

Previous studies have focused on the protective effects of *Lactobacillus reuteri*

C. Liu, J. Bai, M. Li, B. Gu, M. Huang, W. Fu
Department of General Surgery (Hepatopancreatobiliary surgery)
The Affiliated Hospital
Southwest Medical University
Luzhou 646000, China
E-mail: 13141254071@163.com; fuwg@swmu.edu.cn

C. Liu, J. Bai, M. Li, B. Gu, M. Huang, W. Fu
Metabolic Hepatobiliary and Pancreatic Diseases Key Laboratory of Luzhou City
Academician (Expert) Workstation of Sichuan Province
Department of General Surgery (Hepatopancreatobiliary surgery)
The Affiliated Hospital
Southwest Medical University
Luzhou, sichuan 646000, China

T. Cai
School of Medicine
Xiamen University
Xiamen 361100, China

Y. Cheng
Department of General Medicine
West China Hospital
Sichuan University
Chengdu 610000, China

The ORCID identification number(s) for the author(s) of this article can be found under https://doi.org/10.1002/mnfr.202300927

DOI: 10.1002/mnfr.202300927

(*L. reuteri*) against ALD. It has been demonstrated that *L. reuteri* is beneficial for intestinal barrier function and has properties for balancing liver lipid metabolism in ALD.[6,7] To date, the beneficial effects of probiotics on human health are not necessarily directly be attributed to living bacteria but rather to their metabolites or components.[8] According to the International Scientific Association of Probiotics and Prebiotics (ISAPP), inactivated bacteria and/or their metabolites or components that have a beneficial effect on the host.[9] Postbiotic preparations derived from *Lactobacillus* have revealed the presence of numerous bioactive metabolites, such as organic acids and exopolysaccharides.[10,11] Studies have not only demonstrated the safety of postbiotics but have also emphasized their potential benefits in improving gastrointestinal function and managing systemic metabolic responses by regulating gut microbial metabolites.[8,12] These findings imply that postbiotics prepared using *L. reuteri* could represent a novel target for the prevention and treatment of ALD. However, the protective effects of postbiotics derived from *L. reuteri* against ALD and their associated molecular mechanisms are not yet fully understood.

Alcohol consumption disrupts the enterohepatic circulation of bile acids (BAs), which worsens ALD. The Farnesoid X receptor (FXR) serves as a crucial regulator of BA enterohepatic circulation and is predominantly expressed in the liver and intestines. It plays a key role in maintaining BA homeostasis and governing various metabolic processes.[13,14] Activation of intestinal FXR is essential for suppressing BA synthesis and promoting liver regeneration by stimulating the production of fibroblast growth factor 15 (FGF15) in mice. Consequently, FGF15 significantly influences hepatic FXR activation, lipid metabolism, and enterohepatic homeostasis.[15,16] Among the factors influencing FXR signaling, *L. reuteri* has demonstrated efficacy in preventing excessive hepatic lipid accumulation in mice by activating intestinal FXR signaling.[6] Furthermore, the FXR/SHP pathway plays a critical role in regulating fatty acid homeostasis, wherein SHP functions as both a transcriptional repressor and a direct FXR target.[17] Consequently, FXR suppresses the activity of sterol regulatory element-binding protein-1c (SREBP-1c), leading to reduced hepatic triglyceride (TG) levels.[18] These findings hold significant implications for further elucidating the pathophysiological changes and molecular mechanisms of ALD, as well as for the development of new treatments for this condition.

Hence, within the scope of this study, early stages of ALD were induced in both in vivo and in vitro models through ethanol administration. A comprehensive range of methodologies, including network pharmacology analysis, targeted bile acid metabolomics, and histological assessments, were meticulously employed. The primary focus of this study was to elucidate the protective attributes and underlying molecular mechanisms associated with postbiotics derived from *L. reuteri* against ethanol-induced early ALD. Notably, significant attention was devoted to the restoration of intestinal bile acid metabolism and the mitigation of hepatic steatosis. These findings not only provide novel insights into the dynamic interplay between *L. reuteri*-derived postbiotics and ALD but also establish a potential theoretical foundation for the development of innovative therapeutic strategies targeting early ALD in clinical practice.

2. Experimental Section

2.1. Network Pharmacology

The study used network pharmacology to predict the treatment of alcohol-related liver diseases (ALD) using bioactive compounds or metabolites of *L. reuteri*. The process involved the following steps: 1) data collection and collation, including identification of the chemical composition of bioactive compounds or metabolites of *L. reuteri*, screening of candidate compounds, identification of ALD targets, and intersection of the predicted targets of candidate compounds with the disease targets; 2) network topology analysis and protein interaction network construction; 3) enrichment analysis. All retrieved data were obtained as of March 16, 2023.

2.2. Data Collection and Collation

2.2.1. Bioactive Compounds of L. reuteri

It was known that *L. reuteri* metabolized glycerol to produce a special antibacterial substance, reuterin, whose main component was the monomer of 3-hydroxypropionaldehyde (3-HPA).[19] According to a large amount of literature, based on literature search engines such as PubMed (https://pubmed.ncbi.nlm.nih.gov/), and Web of science (https://www.webofscience.com/) for *L. reuteri* related bioactive compounds or metabolites.

2.2.2. Target Gene Prediction for the Selected Chemicals

The simplified molecular input line entry system (SMILES) of the selected bioactive compounds were queried using the PubChem[20] database (https://pubchem.ncbi.nlm.nih.gov/), and then the SMILES of the compounds were entered into the SwissTargetPrediction[21] web tool (http://www.swisstargetprediction.ch/) for target gene prediction, and targets were identified using the probability > 0 as the screening condition.

2.2.3. Target Gene Screening for ALD

Information on known therapeutic target genes associated with ALD was retrieved from the GeneCards[22](https://www.genecards.org/), Gene Expression Omnibus database (https://www.ncbi.nlm.nih.gov/gene), and DisGeNET[23] database (https://www.disgenet.org/).

2.2.4. Venn Analysis

For all of the target genes related with the chosen chemicals and ALD, a Venn diagram was generated for all target genes associated with the bioactive compounds and ALD using Venny 2.1 software showing the intersection of the predicted targets of the bioactive compounds and known targets of the disease.

2.3. Network Topology Analysis and Protein Interaction Network Construction

2.3.1. Network Topology Analysis

Cytoscape 3.9.1 was used to visualize bioactive compounds-target network diagram of *L. reuteri* networks. The study systematically explored the selected bioactive compounds and their potential molecular mechanisms for treating ALD using *L. reuteri* related bioactive compounds or metabolites (postbiotics).

2.3.2. Protein Interaction Network Construction

The target genes obtained from the Venn analysis of intersections were imported into the Multiple Proteins text box in STRING[24] (https://string-db.org/) to construct a protein–protein interaction network (PPI). This network was constructed to systematically understand the protein interactions and identify the most important proteins in the network. Before constructing the PPI network, the organism was set as a common bovine (*Bos taurus*), the minimum interaction score was set to "medium confidence" (0.40), and the unconnected protein nodes were excluded. The constructed PPI network data were mapped using Cytoscape 3.9.1.

2.4. Enrichment Analysis

Gene Ontology (GO) and Kyoto Encyclopedia of Genes and Genomes (KEGG) enrichment analyses were performed using DAVID[25] (https://david.ncifcrf.gov/) bioinformatics resources. The GO analysis included three categories: biological processes (BP), cellular components (CC), and molecular functions (MF). Finally, the bar chart and the Sankey dot pathway enrichment chart were plotted using the Bioinformatics free online platform (www.bioinformatics.com.cn/) for bioinformatics-related data analysis.

2.5. Postbiotics Preparation

For preparation of *L. reuteri*-derived postbiotics,[26] *L. reuteri* was obtained from BioGaia (Sweden) and activated to the third generation in MRS medium. The activated seed solution was inoculated at 2% into the postbiotics preparation medium, where each liter of water contained 20 g glucose, 10 g peptone, 5 g sodium acetate, 4 g yeast extract, 2 g ammonium citrate, 2 g K_2HPO_4-$3H_2O$, 0.2 g magnesium sulfate, 0.1 g $MnSO_4$-H_2O, and 0.05 g manganese sulfate, and was then cultured for 12 h. The resulting fermentation broth was inoculated at 5% in the postbiotics preparation medium and cultured for 21–25 h. Subsequently, the fermentation broth was heat-treated (65 °C, 30 min), sonicated (crushing power 60%, total crushing time 15 min, intermittent time 4 s), and freeze-dried to obtain postbiotics. The postbiotics (derived from *L. reuteri*) and postbiotics preparation media (vehicle) were lyophilized for later use.

2.6. Cell Culture and Treatment

LO2 cells, a normal human liver cell line, were purchased from the Type Culture Collection of the Chinese Academy of Sciences (Shanghai, China). These cells were cultured in Dulbecco's modified Eagle's medium (DMEM; cat# 11965118, Thermo Fisher Scientific, USA) supplemented with 10% fetal bovine serum (FBS; cat# C04001-500, Shanghai XP Biomed Ltd., China) and 1% penicillin–streptomycin (cat# C0222, Beyotime, China). The incubator was maintained at 37 °C with 5% CO_2, and the medium was renewed daily. Experiments were conducted when the cells reached 80–90% confluency after the third generation.

To evaluate the impact of postbiotics on ethanol-induced dysfunction in LO2 cells, the cells were randomly allocated into four groups: control, EtOH, postbiotics, and postbiotics control (vehicle). Cells in the control group were incubated in a normal culture medium for 5 days. Cells in the EtOH group were incubated with normal culture medium for 3 days and then treated with medium containing 150 mM ethanol at a fixed time of the day at 5 pm for an additional 48 h. In the postbiotics group, cells were preincubated with a culture medium containing different concentrations of postbiotics (postbiotics-L: 0.208 mg mL^{-1}, postbiotics-M: 0.3125 mg mL^{-1}, and postbiotics-H: 0.625 mg mL^{-1}) for 3 days, and then incubated in medium containing 150 mM ethanol at a fixed time of the day at 5 pm for an additional 48 h. The vehicle group was identical to the postbiotics group, except that the cells were cultured in a lyophilized postbiotics preparation medium (postbiotics-H: 0.625 mg mL^{-1}). Three to five independent in vitro experiments were conducted, with at least three replicates for each group in every experiment.

Additionally, to investigate the role of farnesoid x receptor (FXR/NR1H4) in ethanol-induced dysfunction in LO2 cells, cells were treated with FXR inhibitors glycine-β-muricholic acid (Gly β-MCA, cat# HY-114392, MedChemExpress, China). Cells were randomly divided into six groups: control, EtOH, postbiotics, control + Gly β-MCA, EtOH + Gly β-MCA, and postbiotics + Gly β-MCA. The control group, EtOH group, and postbiotics group (postbiotics-H: 0.625 mg mL^{-1}) were treated as described previously. In the control + Gly β-MCA group, cells were precultured with 42.954 µM Gly β-MCA for 24 h and then incubated with the normal culture medium for 4 days. In the EtOH + Gly β-MCA group, cells were pretreated with 42.954 µM Gly β-MCA for 24 h, cultured with the normal culture medium for another 48 h, and then cultured with the medium containing 150 mM ethanol at a fixed time of 5 pm for 48 h. In the postbiotics + Gly β-MCA group, cells were pretreated with 42.954 µM Gly β-MCA for 24 h, then incubated with the medium containing 0.625 mg mL^{-1} postbiotics for 48 h, and followed by continued incubation with the medium containing 150 mM ethanol at a fixed time of 5 pm for 48 h. Three to five independent in vitro experiments were conducted, with at least three replicates for each group in every experiment.

2.7. Mouse Strains and Treatments

Wild-type male C57BL/6J mice (8–10 weeks old and without siblings) weighing 20–22 g, were acquired from Luzhou Yinhui Biotechnology Co., Ltd. (Luzhou, China). All mice were housed

under 12 h light/dark cycles in an environment with relative humidity (45–65%) and temperature (22 ± 2 °C), and they had unlimited access to standard rodent diet and water under specific-pathogen-free (SPF) conditions. Prior to the experiments, the mice were allowed to acclimatize for at least 1 week. All animal experiments were conducted in accordance with the "3R" principle (reduce, replace, and reintegrate).

2.8. Establishment of Mouse Ethanol-Induced Liver Injury and Drug Treatment

Chronic-binge alcohol feeding was used to induce alcohol-induced liver injury according to the NIAAA model[27] (three to four technical replicates). Briefly, 42 mice were randomly divided into seven groups of six mice each. Mice in each group were initially fed either a Lieber-DeCarli control diet (TP 4030C, Trophic Animal Feed High-tech Co., Ltd., Nantong, China) or a Lieber-DeCarli EtOH liquid diet (5% vol/vol EtOH, TP 4030D, Trophic Animal Feed High-tech Co., Ltd., Nantong, China). A schematic overview of ALD mouse model and drug treatment was shown in Figure S1, Supporting Information. The detailed grouping was as follows: 1) the control group: Lieber-DeCarli control diet for 28 days; 2) the EtOH group: Lieber-DeCarli control diet for 5 days to adapt to the liquid diet, followed by Lieber-DeCarli EtOH liquid diet for 23 days; 3) the postbiotics (derived from *L. reuteri*) groups: Lieber-DeCarli control diet for 5 days, followed by Lieber-DeCarli EtOH liquid diet for 23 days and gastric perfusion with postbiotics (0.3 g kg^{-1} day^{-1} [postbiotics 30 mg mL^{-1}], 0.6 g kg^{-1} day^{-1} [postbiotics 60 mg mL^{-1}], and 0.9 g kg^{-1} day^{-1} [postbiotics 90 mg mL^{-1}]); 4) the vehicle treated group (the control postbiotics): Lieber-DeCarli control diet for 5 days, followed by Lieber-DeCarli EtOH liquid diet for 23 days and gastric perfusion with the lyophilized postbiotics preparation media (0.6 g kg^{-1} day^{-1}); 5) the Metadoxine group: Lieber-DeCarli control diet for 5 days, followed by Lieber-DeCarli EtOH liquid diet for 23 days and gastric perfusion with metadoxine (11.428 mg kg^{-1} day^{-1}). Postbiotics, postbiotics preparation media (vehicle), and metadoxine were administered to mice by gavage at the appropriate doses dissolved in 0.2 mL of double distilled H_2O (ddH_2O) once daily for 23 days. The control and EtOH groups were administered the same amount of normal ddH_2O. All mice were intragastrically administered a 31.5% v/v ethanol solution (5 g kg^{-1} body weight, alcohol-fed mice) or an equal gavage volume of 45.0% (wt/vol) maltose dextrin (pair-fed control mice) in the morning on day 28th, and all mice were sacrificed 9 h later.

2.9. Sample Collection

Blood samples were collected by heart puncture and centrifuged at 1500 × *g* for 20 min at 4 °C for subsequent biochemical analysis. Serum biochemical indicators were measured using detection kits. The mice were sacrificed by exsanguination after being anesthetized with isoflurane. Liver, jejunum, and colon tissues were harvested. These tissues were divided into two parts: one part was immediately snap-frozen in liquid nitrogen and the other part was fixed in 4% neutral paraformaldehyde.

2.10. Serum and Cellular Supernatant Biochemical Assays

The levels of serum and cellular supernatant alanine transaminase (ALT) (Cat# C009-2-1), aspartate aminotransferase (AST) (Cat# C010-2-1), triglyceride (TG) (Cat# A110-1-1), and total cholesterol (TC) (Cat# A111-1-1) were detected using commercially available detection kits (Nanjing Jiancheng Bioengineering Institute, China) according to the manufacturers' protocols.

2.11. Fibroblast Growth Factor 15 ELISA

Fibroblast growth factor 15 (FGF15) was detected in the serum using mouse fibroblast growth factor 15 (FGF15) enzyme-linked immunosorbent assay (ELISA) kits (MM-44031M1) according to the manufacturer's instructions, which were obtained from Jiangsu Meimian Industrial Co., Ltd., China.

2.12. Real-Time Polymerase Chain Reaction (RT-PCR)

Total RNA extraction was extracted from ileum tissue using FastPure Cell/Tissue Total RNA Isolation Kit (cat# RC101-01, Vazyme, China). Total RNA was subjected to reverse transcription into cDNA by using HiScript III All-in-one RT SuperMix Perfect for qPCR (cat# R333-01, Vazyme, China). Real-time PCR was performed by using ChamQ Universal SYBR qPCR Master Mix (cat# Q711-02, Vazyme, China), and Applied Biosysterms StepOne Real–Time PCR system (Thermo Fisher Scientific, USA). The relative gene expression was determined by the ΔΔCT method. All primer sequences used in this study were provided in Table S1, Supporting Information.

2.13. Histological Analysis

The liver, jejunum, and colon specimens were fixed in 4% neutral paraformaldehyde and embedded in paraffin. Paraffin-embedded sections (5-µm) were stained with hematoxylin and eosin (H&E) (cat# DH0006, Leagene, China). To determine hepatic lipid accumulation, liver sections were embedded in the OCT compound (cat# 4583, SAKURA, Japan). Frozen liver sections (10-µm) were stained with oil red o (ORO) staining (cat# DL0011, Leagene, China), and the percentages of hepatocytes involved in steatosis were assessed by relative lipid content, which was quantified by ImageJ. For ORO staining, red staining was quantified above a preselected threshold, and the average intensities of the images were normalized to the average of all control samples.

2.14. Immunohistochemistry

All colons and jejuna were fixed in 4% neutral paraformaldehyde, embedded in paraffin, and cut into 5-µm sections. The slides were deparaffinized and subjected to antigen retrieval (cat# P0081, Beyotime, China). The slides were rinsed twice with 1× TBS (tris buffered saline, cat# 12498, Cell Signaling Technology, USA) containing 0.025% Triton X-100 (cat# T8200, Beijing Solarbio Science & Technology Co., Ltd., China) for 5 min each

time and blocked in 1% bovine serum albumin in TBS for 2 h at room temperature. Colons were then incubated overnight at 4 °C with rabbit anti-Occludin antibody (cat# ab216327, Abcam, USA) at dilution of 1:100, and rabbit anti-Muc2 antibody (cat# ab272692, Abcam, USA) at dilution of 1:100. And jejuna were incubated overnight at 4 °C with rabbit FXR polyclonal antibody (cat# 25055-1-AP, Proteintech, USA) at dilution of 1:200. The slides were treated with hydrogen peroxide for 15 min before treatment with the biotinylated secondary antibody goat antirabbit IgG H&L (HRP) (cat# ab6721, Abcam, USA) at 1:800 for 1 h at room temperature. The slides were then washed with TBS three times (5 min per time) before treatment with DAB reagent (cat# P0203, Beyotime, China) for 15 min. Counterstaining was performed using hematoxylin, followed by dehydrated in ethanol and green transparent liquid wax (cat# YA0031, Beijing Solarbio Science & Technology Co., Ltd., China).

2.15. Alcian Blue-Periodic AcidSchiff (AB-PAS) Staining

Colons around the most distal fecal pellet in the colon were excised and fixed in 4% neutral paraformaldehyde, embedded in paraffin, sectioned into 5-µm slices, and stained with AB-PAS, which was using AB-PAS staining solution (cat# DG0007, Leagene, China) according to manufacturer's instructions.

2.16. Cellular ORO Staining

Cells in 6-well plates were washed three times with 1× PBS (phosphate-buffered saline, cat# 9872, Cell Signaling Technology, USA) and then stained with ORO staining solution (cat# DL0008, Leagene, China) according to the manufacturer's instructions. Finally, the cells were observed under an inverted fluorescence microscope.

2.17. Protein Expression Analysis

The expression of FXR, FGF15, short heterodimer partner (SHP), sterol regulatory element binding protein-1c (SREBP-1c), platelet glycoprotein 4 (CD36), carbohydrate-responsive element-binding protein (ChREBP), fatty acid synthase (FASN), peroxisome proliferator-activated receptors (PPARα), sodium-dependent bile acid transporter (ASBT), and organic solute transporter beta (OST-β), were evaluated by western blotting analysis. Briefly, the total protein of the liver and ileum tissues and LO2 cells from different groups was isolated in RIPA lysis buffer (cat# 9806S, Cell Signaling Technology, USA) with protease/phosphatase inhibitor cocktail (cat# 5872S, Cell Signaling Technology, USA). After centrifugation of the lysates at 16 000 × g for 15 min at 4 °C, the supernatants were collected and stored at −80 °C until analysis. The concentrations were quantified using the BCA method. Proteins were loaded onto SDS-PAGE (6–10%) gels for electrophoresis and transferred off the separated proteins onto polyvinylidene fluoride membranes (Merck Millipore) using standard procedures. Primary antibodies against FXR (1:3000, cat# 25055-1-AP, Proteintech, USA), FGF15 (1:2000, cat# ab229630, Abcam, USA), SHP (1:4000, cat# 24546-1-AP, Proteintech, USA), SREBP-1c (1:2000, cat# 66875-1-Ig, Proteintech, USA), CD36 (1:1000, cat# 18836-1-AP, Proteintech, USA), ChREBP (1:1000, cat# 13256-1-AP, Proteintech), FASN (1:1500, Abcam ab128856), PPARα (1:800, cat# 15540-1-AP, Proteintech, USA), ASBT (1:500, cat# 25245-1-AP, Proteintech, USA), OST-β (1:300, cat# bs-2128R, Bioss, China), internal control β-actin (1:3000, cat# 20536-1-AP, Proteintech, USA), and GAPDH (1:5000, cat# 10494-1-AP, Proteintech, USA), were incubated with the blots. Horseradish peroxidase-conjugated secondary antibodies (1:10 000, cat# ab6721, cat# ab6789, Abcam, USA) were used, and the blots were incubated for 2 h. After washing with 1× TBST (tris buffered saline with tween 20, cat# 9997, Cell Signaling Technology, USA), protein bands were visualized using a highly sensitive ECL chemiluminescence detection kit (cat# E412-01, Vazyme, China). The band intensities of the proteins of interest were quantified and analyzed using ImageJ software, and all the results were normalized to the corresponding internal control of β-actin or GAPDH for eliminating the variation of the total protein.

2.18. Bile Acid (BA) Quantification

BA in the serum of wild-type mice fed an isocaloric or ethanol-containing diet for 28 days and BA in postbiotics-treated mice were quantified using liquid chromatography-mass spectrometry (LC/MS) as previously described.[28] Briefly, serum samples were extracted in 0.6 mL of methanol (-20 °C) with 100 mg of glass beads, vortex for 60 s. Centrifuge at 12 000 rpm and 4 °C for 10 min, take 0.4 mL of the supernatant and concentrate it to dryness with a vacuum concentrator. Add 0.10 mL of 30% methanol to reconstitute. An appropriate amount of the supernatant was added to the LC-MS bottles. BA separation was achieved using an ACQUITY UPLC BEH C18 column (2.1 × 100 mm, 1.7 µm, Waters, USA) for gas chromatography, and the injection volume was 5 µL, the column temperature was 40 °C. The mass spectrum conditions were electrospray ionization (ESI) source, negative ionization mode, and scans were performed using multiple reaction monitoring (MRM).[29]

2.19. Quantitative and Qualitative Analysis of Postbiotic Components

The lyophilized postbiotics (derived from *L. reuteri*) and postbiotics preparation media (vehicle) were qualitatively and quantitatively analyzed using UHPLC-MS[30] as previously described. Briefly, the LC/MS system used a Shimadzu Nexera X2 LC-30AD with an Acquity UPLC HSS T3 column (1.8 µm, 2.1 × 50 mm, Waters) and a triple quadrupole mass spectrometer (5500 QTRAP, AB SCIEX). Metabolites were detected in both negative and positive ionization modes. Samples of 5 µL were injected sequentially with an LC autosampler. The Acquity UPLC HSS T3 column was set at 40 °C with a flow rate of 200 µL min^{-1} and a gradient of 0.1% formic acid in water (solvent A) and 100% acetonitrile (solvent B). The gradient started at 100% solvent A for 2.5 min, increased to 70% solvent A over 9 min, then decreased to 0% solvent A over 1 min, with a 5.4 min hold before re-equilibrating. QC samples were injected periodically.

For negative-ionization mode, the source temperature was 550 °C, with GAS1 at 40, GAS2 at 50, CUR at 35, and ISVF at -4500 V. In positive-ionization mode, the source temperature was 550 °C, with GAS1 at 40, GAS2 at 50, CUR at 35, and ISVF at 5500 V. Transitions were monitored using MRM mode. Moreover, for data preprocessing and filtering, MultiQuant 3.0.2 software was used to extract the original MRM data of MT1000 KIT metabolites and obtain the peak area of each metabolite.

2.20. Statistical Analysis

Results were expressed as mean ± SEM. (unless otherwise stated). The Shapiro–Wilk test was used to test the normality of the samples. Differences among groups were analyzed using a one-way analysis of variance (ANOVA). When significance was achieved, Duncan's multiple comparisons tests were conducted to identify the sources of the differences. Statistical analyses were performed using GraphPad Prism v8.2.1. A $p < 0.05$ was considered to be statistically significant.

3. Results

3.1. Identification and Prediction of Bioactive Compounds from *L. reuteri* (Postbiotics), with Target Enrichment Analysis for Postbiotics-ALD

Fourteen bioactive metabolites of *L. reuteri* (postbiotics) were identified in PubMed and Web of Science and screened using the PubChem web tool (**Figure 1a**). The gastrointestinal absorption of the compounds was not considered, as it is not known which means *L. reutei* and its metabolites act. By intersecting these metabolites with the ALD targets, 156 relevant targets were identified (Figure 1b). A protein–protein interaction network was constructed using the STRING database and Cytoscape, the nodes in the network were ranked according to the magnitude of the degree value, and the top 23 proteins with the highest connectivity were selected (Figure 1c). The GO enrichment analysis included three biological aspects, revealing that many targets were involved in the biological processes (BP) regulation of gene expression, apoptotic process, and cellular response to epidermal growth factor stimulus. The cellular components (CC) results showed that the targets were localized in the presynaptic membrane, extracellular space, and region, while the MF results showed that most targets were associated with identical protein and enzyme binding (Figure 1d). KEGG pathway analysis indicated that lipids, atherosclerosis, and alcoholism were associated with the key targets (Figure 1e). These results suggest that FXR may be a potentially important target for postbiotics in the treatment of ALD.

3.2. Postbiotics Alleviated Ethanol-Induced Hepatocellular Steatosis In Vitro

Steatosis is a primary pathological feature of ALD.[5] To investigate the potential protective effects of postbiotics on ALD, LO2 cells were subjected to a hepatocellular model of early ALD in vitro by treating with EtOH (150 Mm, 48 h). As expected, compared to the control group, EtOH-treated cells exhibited a significant increase in lipid droplets ($p < 0.05$, **Figure 2d,e**) and elevated levels of TG, ALT, and AST ($p < 0.001$, Figure 2a–c), indicating a disruption in lipid homeostasis and cellular injury. However, treatment with postbiotics-H and postbiotics-M significantly ameliorated ethanol-induced hepatocellular lipid accumulation and cell injury ($p < 0.05$, Figure 2a–e). These findings indicate that postbiotics may have the potential to mitigate the pathological processes associated with ALD.

3.3. Postbiotics Suppressed Ethanol-Induced Liver Injury in ALD Mice

In this study, we established an ALD model in C57BL/6J mice using the NIAAA method and administered different doses of postbiotics (0.3, 0.6, and 0.9 g kg^{-1} day^{-1}) via gavage for 23 days. Our findings demonstrated that postbiotics-treated mice exhibited decreased liver weight and liver-to-body mass ratios compared to ethanol-fed and vehicle-treated mice after Lieber-DeCarli EtOH liquid diet feeding ($p < 0.01$, **Figure 3a,b**). Additionally, postbiotics treatment mice showed liver lesion reversal, as evidenced by H&E staining, with reduced liver lipid droplet accumulation and decreased serum ALT and AST levels ($p < 0.05$, Figure 3c–e). These protective effects were comparable with those observed in mice treated with metadoxine, a commonly used positive control for studying hepatoprotective drugs.[31] These results suggested that postbiotics have the potential to ameliorate ethanol-induced liver injury in mice.

3.4. Postbiotics Alleviated Hepatic Steatosis in ALD Mice

To assess the impact of postbiotics on ethanol-induced hepatic steatosis, we used serum levels of triglycerides (TG) and total cholesterol (TC), along with oil red O (ORO) staining. Remarkably, postbiotics administration led to a significant reduction in hepatic lipid accumulation, as indicated by the lower serum TG and TC levels in postbiotics-treated mice ($p < 0.05$, **Figure 4a,b**). Additionally, ORO staining demonstrated a significant decrease in liver lipid accumulation in postbiotic-treated mice after ethanol exposure compared to ethanol-treated mice ($p < 0.01$, Figure 4c,d). Collectively, these findings strongly suggested that postbiotics can mitigate ethanol-induced hepatic steatosis.

3.5. Postbiotics Regulated Intestinal FXR-Mediated BA Metabolism in ALD Mice

Hepatic lipid metabolism is intricately linked to the enterohepatic circulation of BAs, which is regulated by the key factor FXR.[32] The ASBT in the ileum reabsorbs BAs, activating intestinal FXR, which induces IBABP for intracellular transport of BAs to OSTα/β for excretion, leading to the excretion of BAs into the portal circulation.[16,32] To investigate the role of intestinal FXR in regulating the intestinal BAs and its contribution to ALD, we conducted an immunohistochemical analysis and found a decrease in FXR expression in the jejunum of ethanol-fed mice,

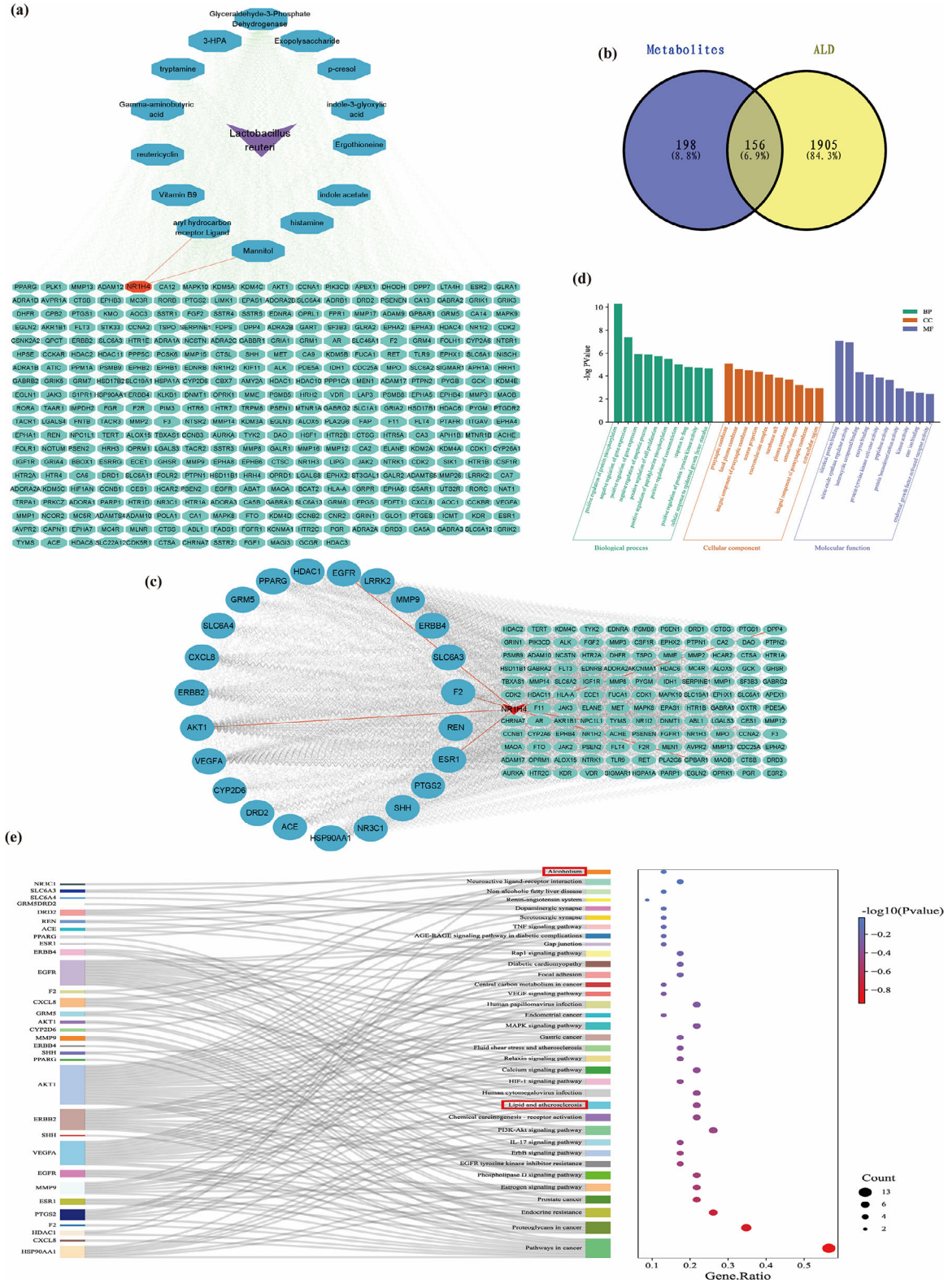

Figure 1. Identification of postbiotics derived from *L. reuteri*, construction of PPI network, GO, and KEGG analysis results of key targets in postbiotics. a) Bioactive compounds-target network diagram of *L. reuteri*. b) Veen map of bioactive compounds of *L. reuteri* and ALD target genes. c) Protein–protein interaction (PPI) network of targets. d) Histogram of GO function analysis of key targets. e) Sankey dot plot chart of KEGG enrichment analysis of key targets.

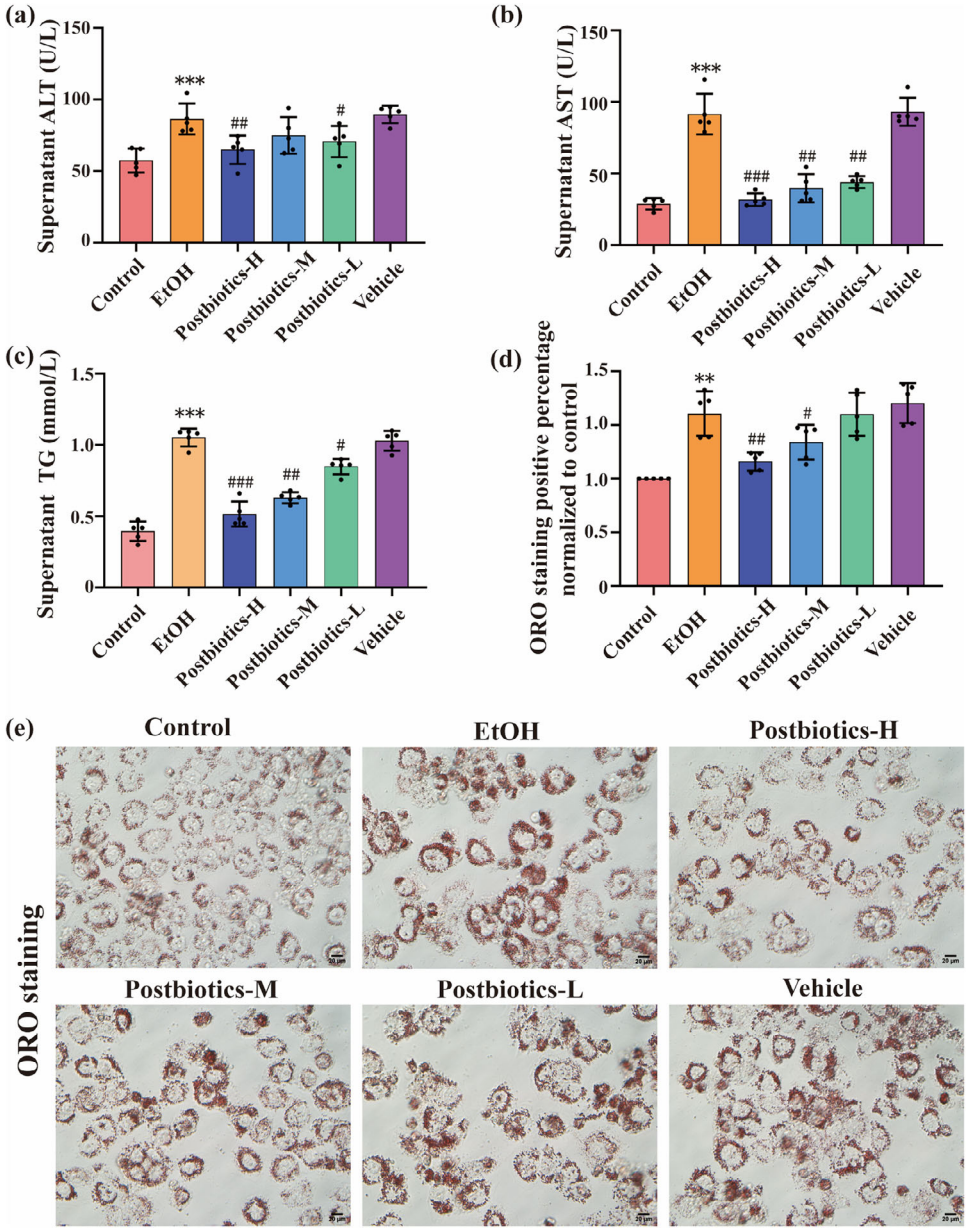

Figure 2. Postbiotics reduced hepatocellular lipid accumulation in LO2 cells stimulated by ethanol. a–c) The levels of ALT, AST, and TG in cell supernatant, respectively. d) Quantitative results of ORO staining amount six groups. e) Representative images of oil red O (ORO) staining (scale bars, 20 μm) of different treated groups in LO2 cells ($n = 5$ replicates for each group) (compared to the control group, $^{**}p < 0.05$, and $^{***}p < 0.001$; compared to the EtOH group, $^{\#}p < 0.05$, $^{\#\#}p < 0.01$, and $^{\#\#\#}p < 0.001$).

which was significantly increased by postbiotics treatment ($p < 0.05$, **Figure 5a**). **Figure 6** illustrates the mRNA and protein expression of bile acid metabolism-related genes in the ileum. The expression levels of ASBT, IBAPB, OST-β, and FXR, representing BA transporters, showed an anomalous alteration in EtOH-fed mice, which was significantly mitigated by postbiotics ($p < 0.05$, Figure 5c–e).

BAs activate FXR in intestinal cells, leading to the secretion of FGF15, which then circulates to the liver through the portal vein to suppress bile acid synthesis. FXR-FGF15 signaling plays a crucial role in liver FXR activation, hepatic lipid metabolism, and enterohepatic homeostasis.[16,33] Our findings showed that postbiotics treatment resulted in elevated serum FGF15 levels and ileum FGF15 mRNA and protein expression ($p < 0.01$, Figure 5b–e), indicating strengthened FGF15 signaling in enterohepatic circulation, which may be involved in the beneficial effects of postbiotics on intestinal integrity promotion. Therefore, postbiotics may regulate FXR signaling-mediated bile acid metabolism in vivo, activating the FXR/FGF15 signal and influencing the enterohepatic circulation of bile acids. These results suggest that postbiotics have a regulatory effect on intestinal FXR signaling-mediated BAs metabolism.

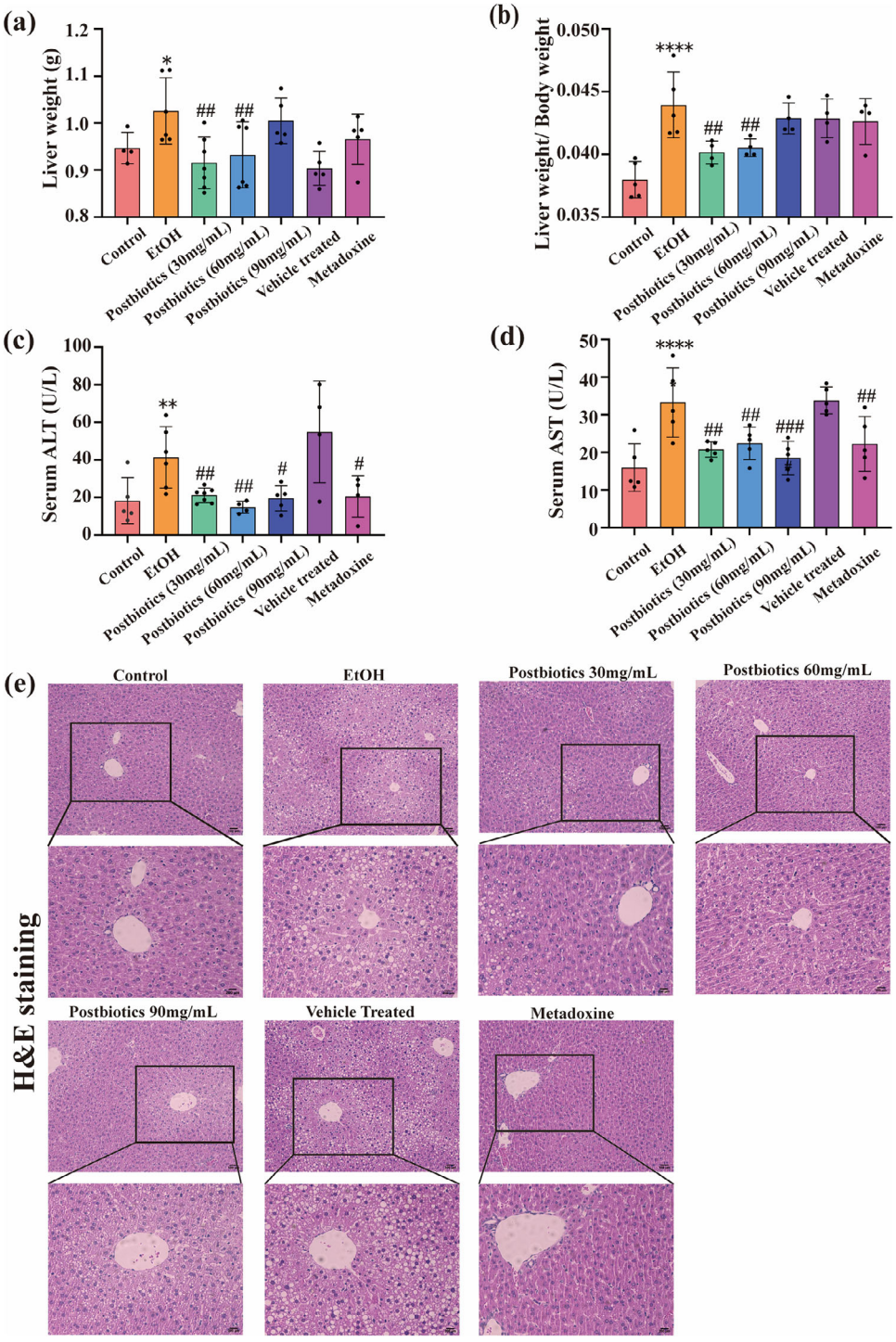

Figure 3. Postbiotics protected mice from ethanol-induced liver injury. a, b) Measurements of the body weight, the ratio of liver weight to body weight (LW/BW). c, d) The levels of serum ALT and AST in different groups. d) Representative images of H&E staining in liver sections from different groups (n = 4–7 mice per group, 100× and 200× magnification) (compared to the control group, $^{*}p < 0.05$, $^{**}p < 0.01$, and $^{****}p < 0.0001$; compared to the EtOH group, $^{\#}p < 0.05$, $^{\#\#}p < 0.01$, and $^{\#\#\#}p < 0.001$).

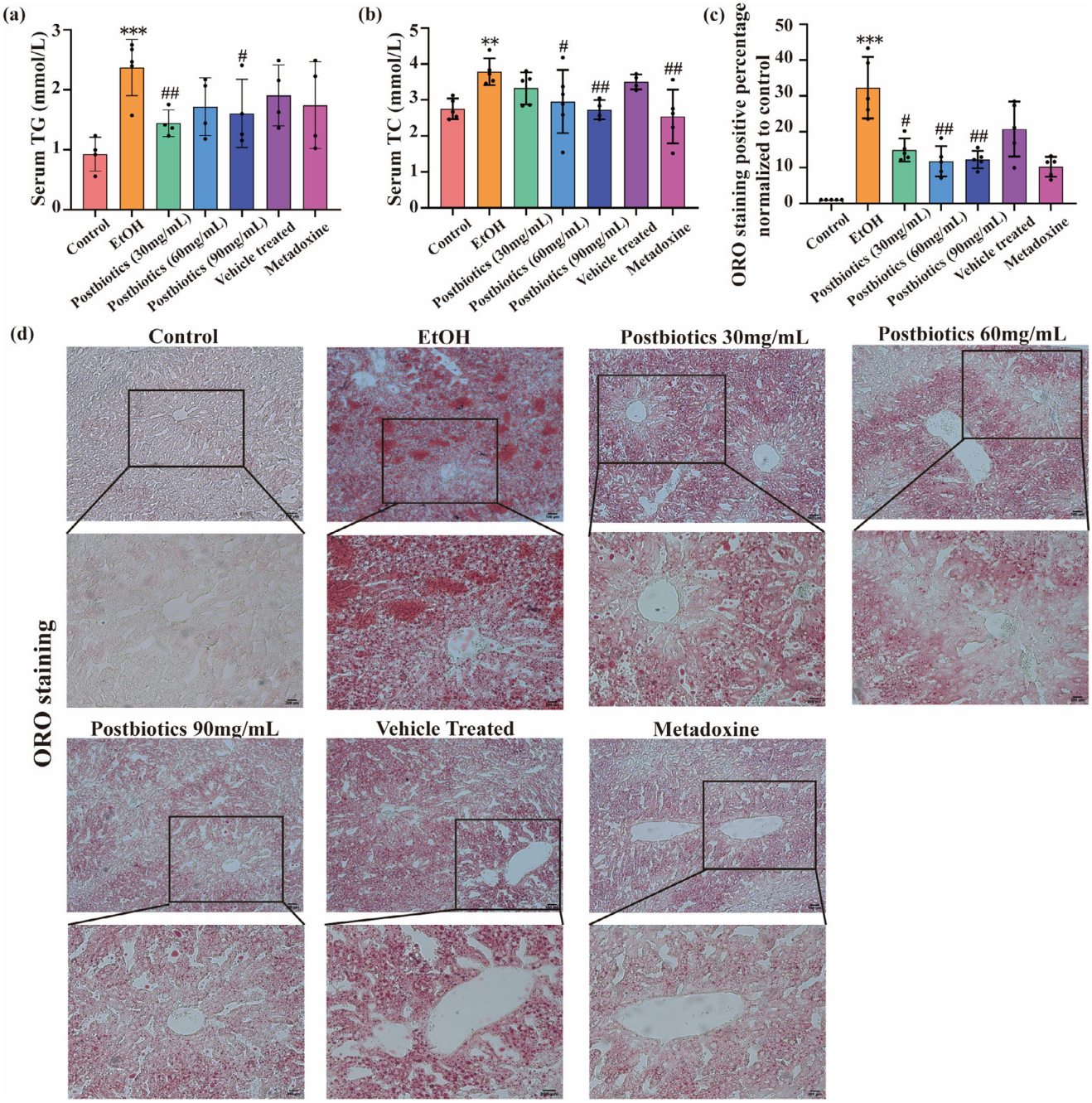

Figure 4. Postbiotics attenuated hepatic steatosis in ALD mice. a, b) The levels of serum triglyceride (TG) and total cholesterol (TC) in different groups. c) Results for ORO-positive staining were analyzed and quantified. d) Representative images of ORO staining in liver sections under different treatments (n = 4–6 mice per group, 100× and 200× magnification) (compared to the control group, $^{**}p < 0.01$, and $^{***}p < 0.001$; compared to the EtOH group, $^{\#}p < 0.05$, $^{\#\#}p < 0.01$, and $^{\#\#\#}p < 0.001$).

3.6. Postbiotics Modulated the Serum Bile Acids Composition

Chronic ethanol intake disrupts the balance of bile acid metabolism, leading to elevated systemic BAs levels and increased levels of secondary BAs.[33,34] To investigate the effects of postbiotics on BAs metabolism, we performed a targeted analysis of BAs composition by using a validated method.[35] Consistent with previous results,[36] we found that ethanol-fed mice had altered total serum BAs and a modified composition with elevated levels of secondary BAs. Notably, the postbiotics changed the alterations induced by chronic ethanol administration ($p < 0.05$, Figure 6d–g). Furthermore, separation was observed among the control, ethanol, and postbiotics groups for the serum samples analyzed using the PCA and OPLS-DA score plots (Figure 6a–c). The metabolic upstream and downstream relationships among the detected substances based on the KEGG database are

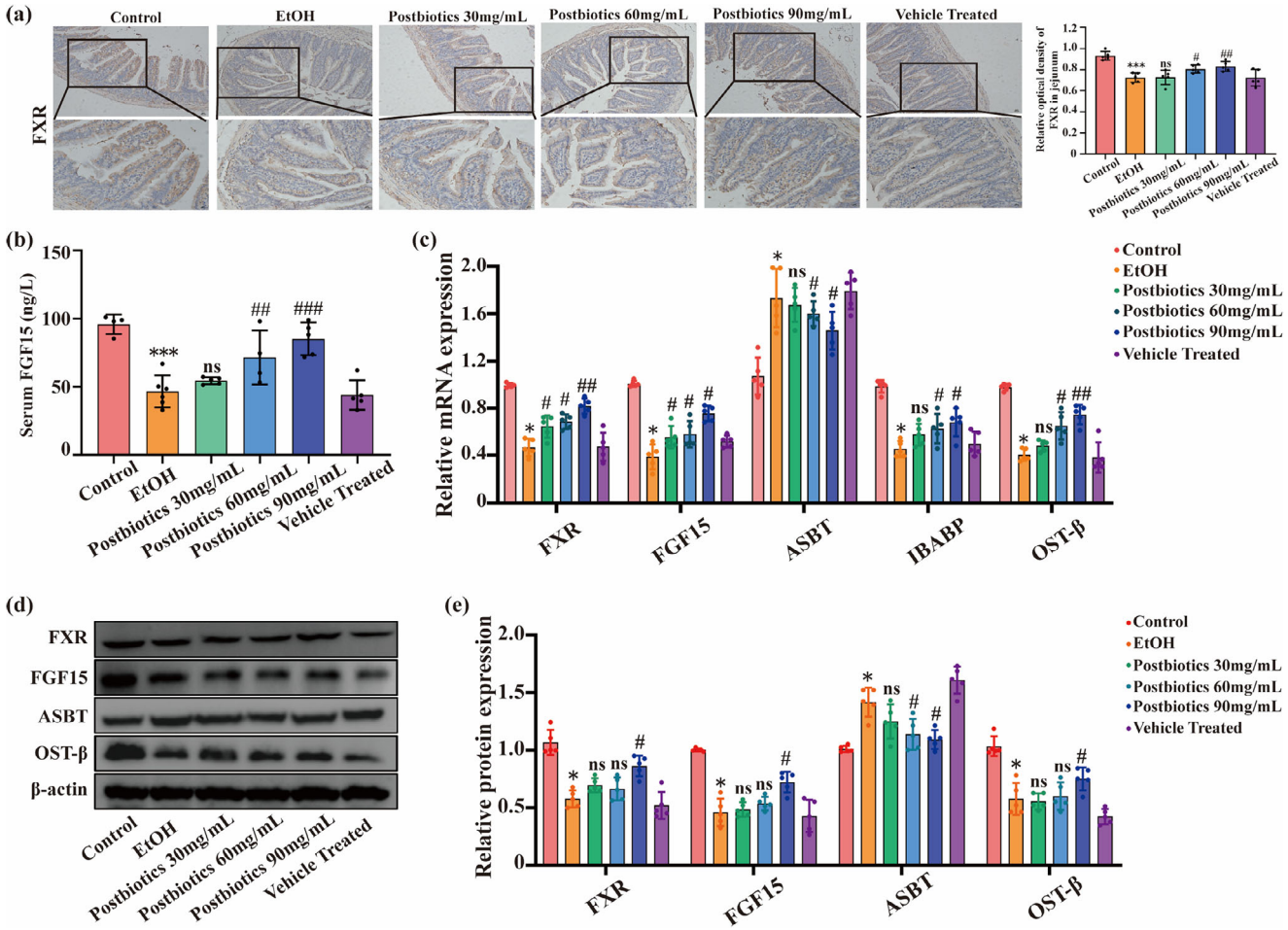

Figure 5. Postbiotics modulated intestinal FXR-mediated BAs metabolism and increased FGF15 levels in the serum of ALD mice. a) Immunohistochemistry results of FXR in the jejunum. b) The levels of serum FGF15 in different groups. c–e) Ileal relative mRNA and protein expression of gene involved in BA regulation and transport ($n = 4$–6 mice per group, 100× and 200× magnification) (compared to the control group, $^{*}p < 0.05$, and $^{***}p < 0.001$; compared to the EtOH group, $^{\#}p < 0.05$, and $^{\#\#}p < 0.01$; *ns*: no significance).

presented in Figure S2, Supporting Information. These results suggest that postbiotics may alter the disrupted BAs metabolism during chronic ethanol administration by modulating total BAs pool composition and decreasing secondary BAs levels.

3.7. Postbiotics Activated the FXR/SHP/SREBP1c Axis Both In Vivo and In Vitro

Ethanol consumption has been shown to disrupt hepatic lipid homeostasis.[37] To better understand the molecular mechanism underlying the postbiotics-lowering effect on hepatic steatosis, we used western blotting to measure the hepatic protein levels of several important proteins involved in lipid homeostasis in mice. Intriguingly, both in vivo and in vitro alterations were associated with modulations of SREBP-1c, CD36, ChREBP, and FASN expression; however, PPAR-α expression displayed a reverse pattern in vivo ($p < 0.05$, **Figure 7a–f**). Because these genes are regulated by FXR[6,38] we further measured the protein expression of FXR and its downstream target gene, SHP. As expected, both in vivo and in vitro experiments showed that the postbiotics increased FXR expression and subsequently regulated SHP expression ($p < 0.05$, Figure 7a,b,d,e). These results indicate that postbiotics may ameliorate ethanol-induced hepatic steatosis by regulating the FXR/SHP/SREBP-1c axis.

3.8. Inhibition of FXR Activation Attenuated the Protective Effects of Postbiotics in ALD

Based on these findings, we propose that postbiotics exert beneficial effects on ALD by activating the FXR signaling pathway. To test this hypothesis, we employed Gly β-MCA to inhibit FXR activation in LO2 cells. Our results showed that postbiotics effectively mitigated ethanol-induced lipid accumulation in LO2 cells, as confirmed by ORO staining and TG analysis of the cell supernatants. Notably, the protective effect of postbiotics was abolished by Gly β-MCA treatment ($p < 0.01$, **Figure 8a–c**). In summary, we found that the protective effect of postbiotics against hepatic steatosis in ALD was dependent on FXR activation.

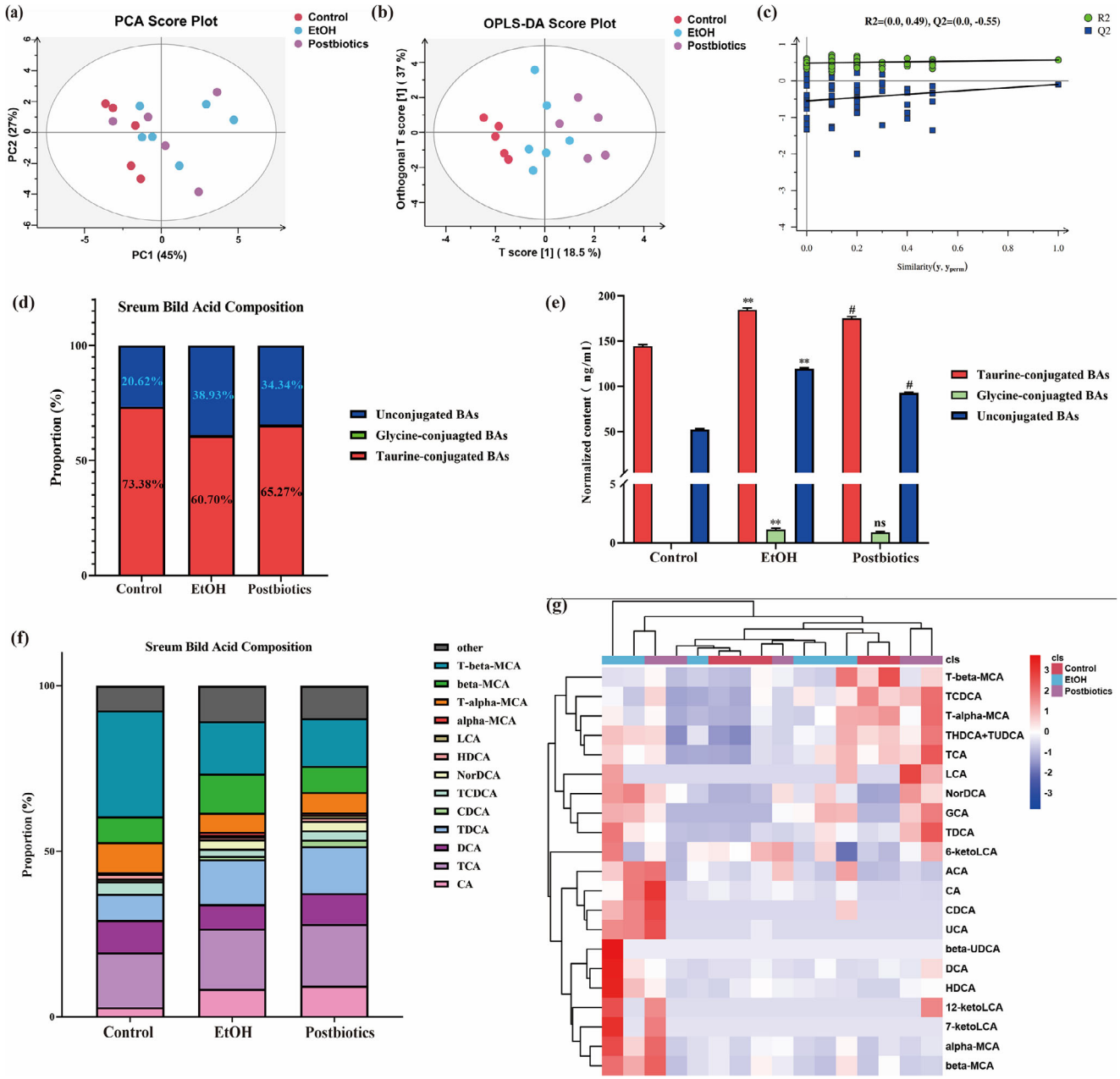

Figure 6. Postbiotics changed the BAs species in the serum of ethanol-induced mice. a–c) Score plot of PCA and OPLS-DA, and permutation test of the OPLS-DA model for different treatment groups. d, f) Bile acid composition ratio in serum contents from control, EtOH, and postbiotics (postbiotics 90 mg mL^{-1}) groups. e) The total amount (ng mL^{-1} dried weight of stool) of taurine-conjugated bile acids, glycine-conjugated bile acids, and unconjugated bile acids in serum among control, EtOH, and postbiotics groups, respectively. g) The heatmap showed the relative variations of serum bile acids (other: other bile acids; compared to the control group, $^{**}p < 0.01$; compared to the EtOH group, $^{\#}p < 0.05$; *ns*: no significance).

3.9. Identification and Analysis of Functional Metabolites in Postbiotics

Functional metabolites in postbiotics were detected using UHPLC-MS. Separation was observed among the control, ethanol, and postbiotics groups for the serum samples analyzed using the PCA and OPLS-DA score plots (**Figure 9a–c**). With OPLS-DA model VIP > 1 and p value <0.05 as the screening criteria, the metabolites with significant differences were screened and their expression changes were analyzed. The metabolites screened for significant differences between postbiotics and Vehicle were mainly concentrated in Flavonoids, benzene, and substituted derivatives, Amino acids, peptides, analogues, and Bile acids, etc. (Figure 9d).

Building upon our previous observations, postbiotics has been identified as a potential agent in mitigating ALD through the activation of FXR signaling. FXR is a crucial regulator responsive to BAs, acting as an endogenous ligand. Activation of FXR induces

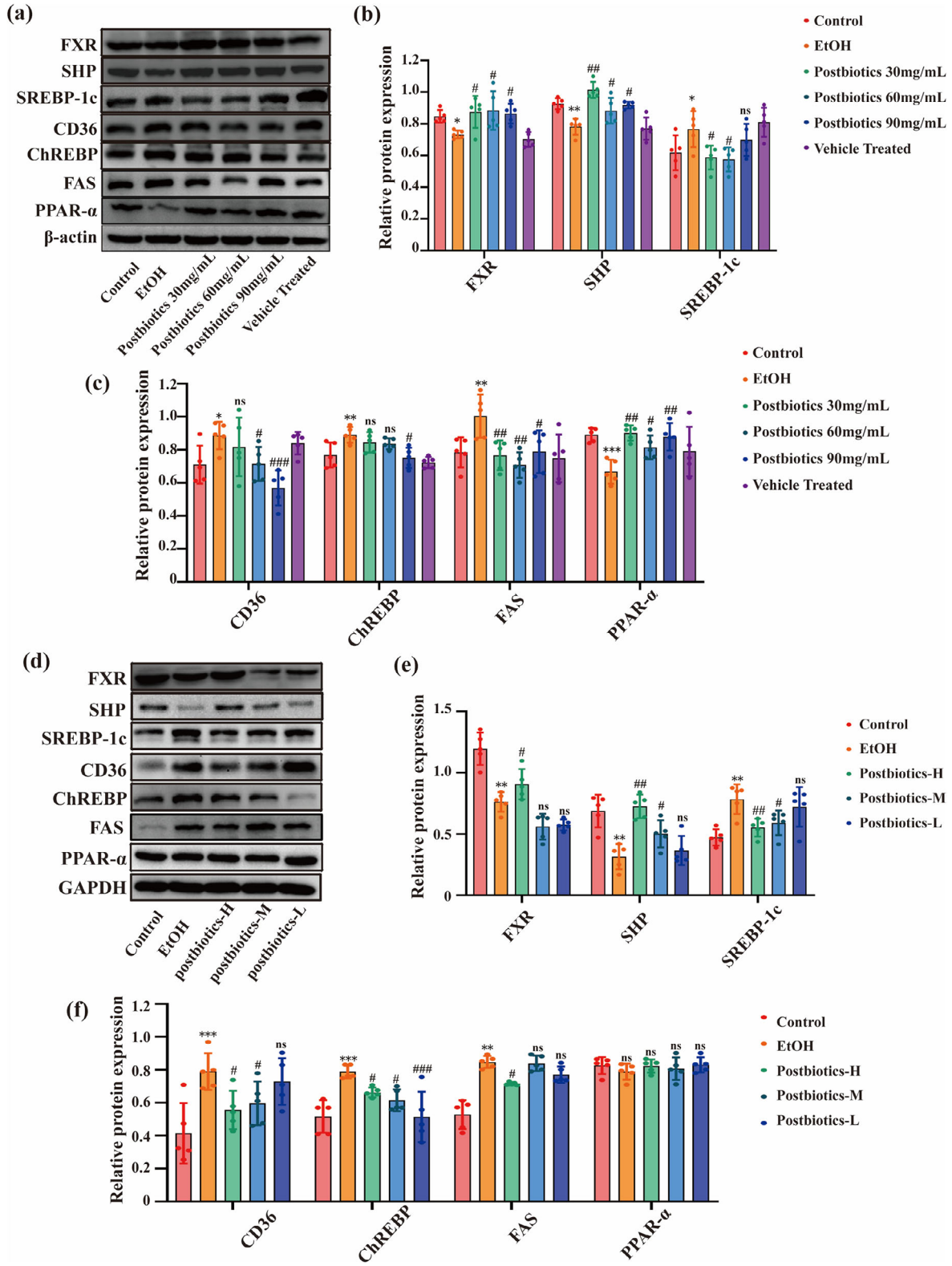

Figure 7. In vivo and in vitro, postbiotics upregulated protein expression of FXR and SHP, but downregulated protein expression of hepatic lipogenic markers (SREBP-1c, CD36, and ChREBP). a–c) Representative western blotting and quantification of the protein expression of total FXR, SREBP1-c, SHP, CD36, ChREBP, FASN, and PPAR-α in the liver of the indicated groups of mice. d–f) Representative western blotting and quantification of the protein expression of total FXR, SREBP1-c, SHP, CD36, ChREBP, and PPAR-α in LO2 cells of the indicated groups ($n = 5$ per group) (compared to the control group, $^{*}p < 0.5$, $^{**}p < 0.01$, and $^{***}p < 0.001$; compared to the EtOH group, $^{\#}p < 0.05$, $^{\#\#}p < 0.01$, and $^{\#\#\#}p < 0.001$; *ns*: no significance).

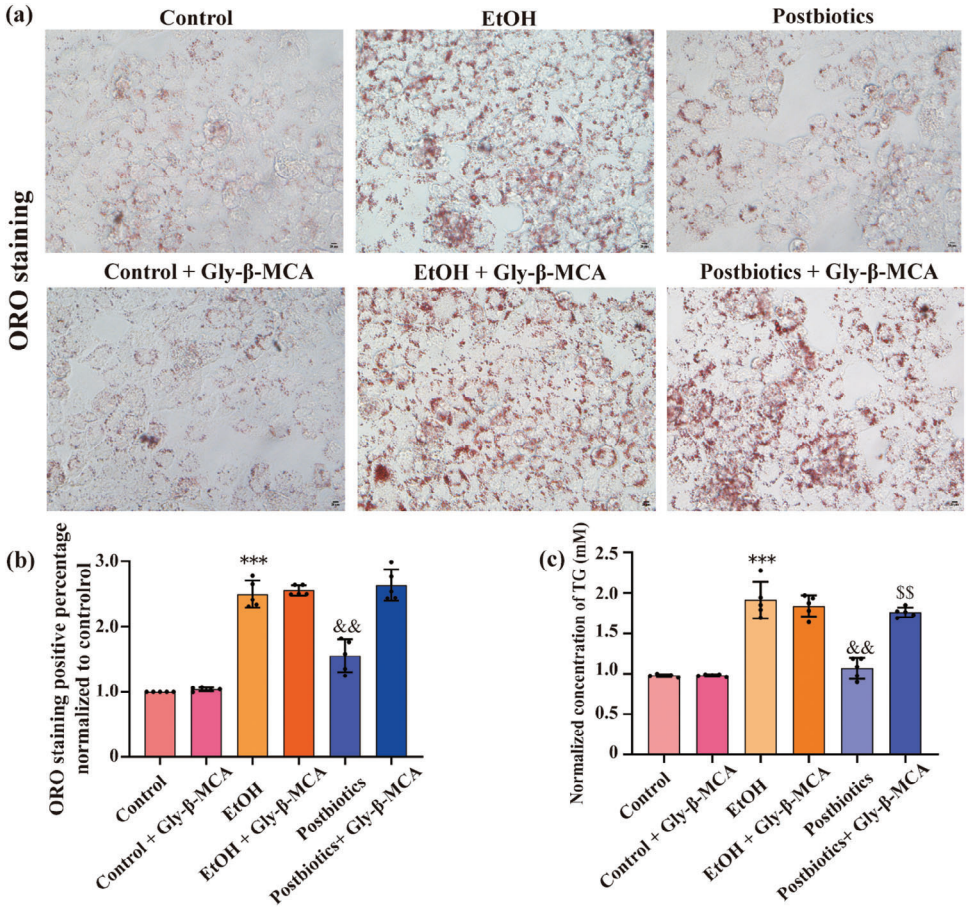

Figure 8. The anti-ALD effect of postbiotics was dependent on FXR activation. a, b) Representative images and quantitative results of ORO staining (scale bars, 20 μm) of different treated groups in LO2 cells. c) The levels of cell supernatant TG in different groups ($n = 5$ replicates for each group) (compared to the control group, $^{***}p < 0.001$; compared to the EtOH group, $^{\&\&}p < 0.01$; compared to the postbiotics group, $^{\$\$}p < 0.01$).

the transcription of genes involved in BAs metabolism/transport, lipid and glucose metabolism, thus contributing to the equilibrium of these essential substances and influencing various pathological processes.[39] Subsequently, we conducted a detailed analysis of BAs within the postbiotics, revealing specific endogenous BAs that modulate FXR activation[39,40] notably 23-Nordeoxycholic acid ($p < 0.05$), deoxycholic acid ($p = 0.17$), lithocholic acid ($p = 0.27$), and cholic acid ($p = 0.28$) (Figure 9e,f). These results suggest that the anti-ALD effects of Postbiotics may be mediated through FXR activation by endogenous BAs.

4. Discussion

Excessive alcohol consumption causes liver histopathological changes and dysfunction. ALD is characterized by excessive lipid accumulation in the liver due to alcohol abuse. Steatosis, marked by the buildup of triglycerides and cholesterol esters in hepatocytes, is strongly associated with the progression of advanced stages of ALD.[37,41] Studies have demonstrated the potential of *L. reuteri* in alleviating ALD; however, it is uncertain whether postbiotics derived from *L. reuteri* can also protect against ALD and the associated molecular mechanisms. In our current study, hepatic steatosis was induced by ethanol in vivo[27] and in vitro.[42] Our findings indicate that postbiotics derived from *L. reuteri* effectively mitigated steatosis in ethanol-treated mice and L02 cells. Nonetheless, the specific molecular mechanisms underlying the effects of postbiotics on lipid regulation in ALD remain unclear.

Furthermore, we employed network pharmacology to predict the efficacy of postbiotics against ALD while exploring the underlying mechanisms. Network pharmacology offers a comprehensive perspective on the molecular-level interactions between components and diseases[43,44] allowing for a theoretical and scientific basis to investigate the effectiveness of postbiotics in treating ALD. In this study, integrating network pharmacology, we identified the major bioactive metabolites (postbiotics) in *L. reuteri* and their primary targets in ALD, which may exert therapeutic effects. Interestingly, we revealed that postbiotics reduced hepatic steatosis both in vivo and in vitro, and we observed that FXR serve as a potential target for the two bioactive metabolites of *L. reuteri*, potentially exerting protective or harmful effects on ALD. Additionally, key targets associated with lipids, atherosclerosis, and alcoholism in the KEGG database were identified. These findings suggest that FXR stands as a potential therapeutic target for mitigating the progression of ALD.

FXR, which is primarily expressed in the liver and intestines, is an important regulator of bile acid (BA) enterohepatic circulation.

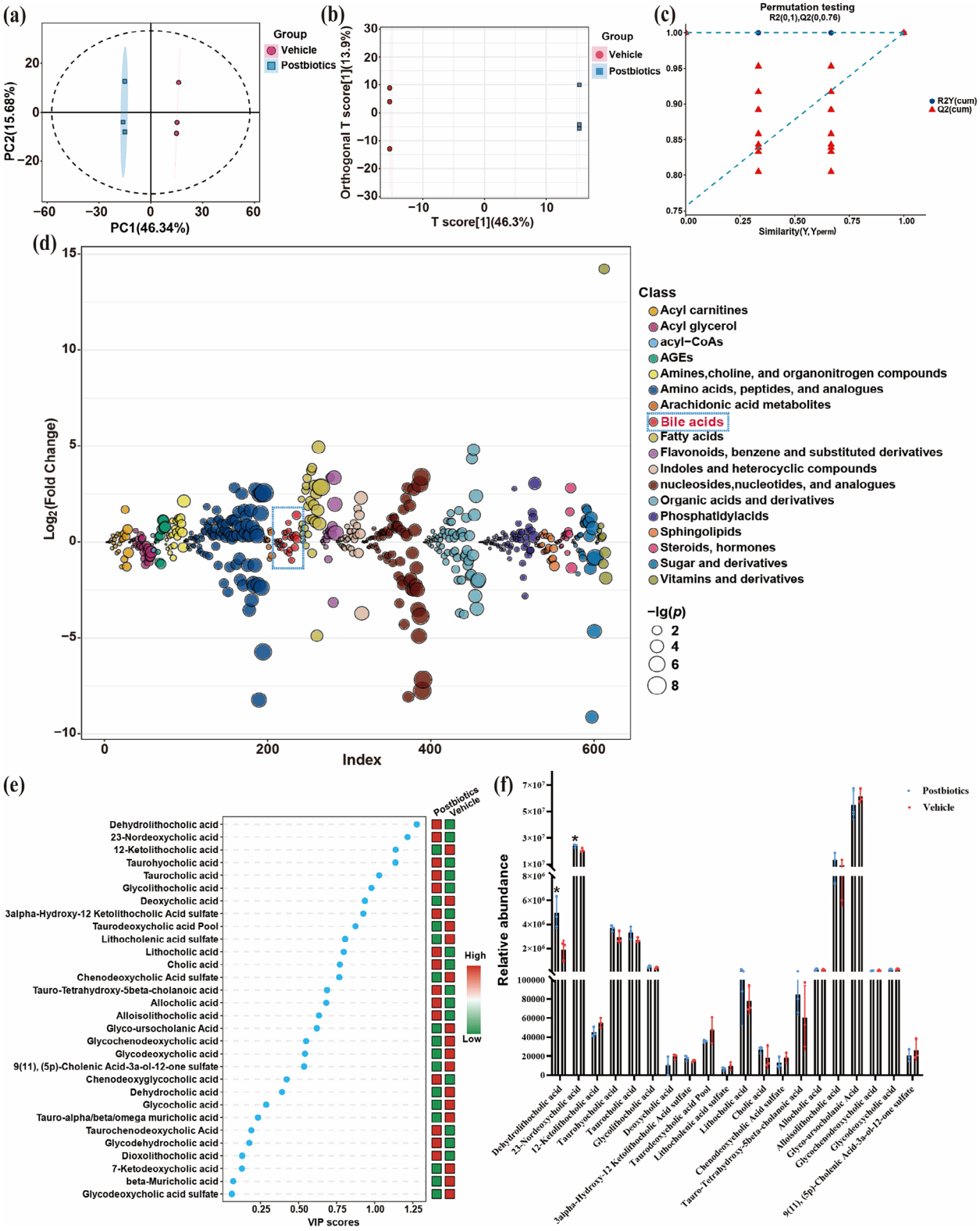

Figure 9. Detection and analysis of functional metabolites in postbiotics. a–c) Score plot of PCA and OPLS-DA, and permutation test of the OPLS-DA model for postbiotics and vehicle. d) Postbiotics versus Vehicle comparison group FC and *p*-valued bubble plots. Each circle represents a metabolite, and the larger the circle, the greater the negative logarithmic transformation of *p*-value, that is, the higher the significance. Different colors indicate primary classes, with metabolites of the same class arranged together. e,f) BAs metabolic VIP value map and its relative abundance in postbiotics and Vehicle. The higher the VIP value, the greater the contribution of the metabolite to the sample classification (compared to the Vehicle group, $*p < 0.05$).

And hepatic lipid metabolism is closely tied to the enterohepatic circulation of bile acids, a process regulated by the key factor FXR. Studies have revealed that alcohol disrupts the enterohepatic circulation of BAs in both mice and humans and that FXR deficiency in mice exacerbates ALD.[45,46] The ileal brush-border membrane transporter ASBT reabsorbs bile acids, triggering the activation of intestinal FXR. This activation induces IBABP to bind with bile acids, potentially facilitating the intracellular transport of bile acids to the basolateral membrane-localized OSTα/β, ultimately resulting in the excretion of bile acids into the portal circulation.[32,34] Additionally, FXR in the liver acts through a feedback repression mechanism by inducing SHP expression, which allows the liver to downregulate BA synthesis in response to maintaining a constant BA pool[47] and intestinal FXR is critical in suppressing BA synthesis and promoting liver regeneration by strongly inducing the expression of FGF15 in mice.[33] FGF15 plays critical roles in hepatic FXR activation, lipid metabolism, and enterohepatic homeostasis.[33,48] Consistent with our results, postbiotics restored disrupted BA homeostasis, upregulated SHP expression, and normalized serum FGF15 levels in alcohol-treated mice. Moreover, the postbiotics increased the expression of hepatic and intestinal FXR. These results imply that the protective effects of postbiotics may be partly mediated by regulation of BA metabolic dysfunction. In addition, FXR in intestinal epithelial cells plays a vital role in sensing intracellular bile acid levels and participating in intestinal bile acid metabolism, which helps maintain intestinal barrier integrity.[49,50] Our results showed that postbiotics may modulate bile acid metabolism in vivo by regulating FXR signaling, activating the FXR/FGF15 pathway, and influencing the enterohepatic circulation of BAs. Moreover, postbiotics enhanced intestinal barrier integrity by promoting Muc2 and occludin expression and boosting the regeneration of goblet cells, maintaining normal structural and function integrity of the gut (Figure S4, Supporting Information). In summary, these results show that postbiotics regulate intestinal FXR expression and serum FGF15 levels by ameliorating alcohol-induced BA pool disruption which is essential for maintaining intestinal microecology, liver metabolic homeostasis.

In addition to bile acid metabolism, both FXR and SHP have been reported to regulate fatty acid homeostasis. SHP is both a transcriptional repressor and a direct FXR target.[38,51] Activated by bile acids in the liver, FXR crucially regulates hepatic lipid metabolism by activating SHP. This leads to the suppression of SREBP-1c expression, resulting in decreased synthesis of key enzymes in the fatty acid biosynthesis pathway and notable impacts on overall hepatic lipid metabolism. The FXR/SHP/SREBP-1c signaling pathway stands out as a central regulatory axis in the intricate management of hepatic lipid metabolism.[17,38,51] Moreover, FXR activation inhibited hepatic de novo lipogenesis and promoted fatty acid β-oxidation by inducing PPAR-α expression, thus limiting hepatic lipid accumulation.[36] Consistent with our findings, postbiotics reversed the effect of alcohol treatment on SHP, SREBP-1c, and PPAR-α expression, while no changes in PPAR-α were observed in vitro. Additionally, both in vivo and in vitro, postbiotics restored the protein expression alterations associated with lipid accumulation, including CD36, ChREBP, and FASN, which were mediated by FXR. Furthermore, we used Gly β-MCA to block the activation of the FXR to investigate the role of FXR in postbiotics reducing ALD. ORO staining and cell supernatant TG results revealed that postbiotics reduced ethanol-induced lipid accumulation in LO2 cells that was eliminated by Gly β-MCA treatment, suggesting that the protective effect of postbiotics on hepatic steatosis was dependent on FXR activation.

Our previous experiments demonstrated that *L. reuteri* effectively mitigated intestinal and hepatic damage in ALD mice by activating the FXR signaling.[6] However, the beneficial effects of probiotics on host health may not be directly attributed to live bacteria. Instead, it could be the result of postbiotics, which are the metabolic byproducts or cellular components of live bacteria. Postbiotics, the fourth generation of microbiome products, modulate the gut microbiota, improving gastrointestinal function and systemic metabolism.[8,10] Published literature review revealed that *L. reuteri* contains bioactive metabolites similar to prebiotics, such as 3-HPA,[19] Ergothioneine,[52] and aryl hydrocarbon receptor ligands[53] suggesting their potential involvement in the anti-ALD process, which requires further research and confirmation.

In this study, we employed UHPLC-MS to detect and analyze the functional metabolites of postbiotics. Significant differences were observed in metabolite profiles, including flavonoids, benzene derivatives, amino acids, peptides, analogues, and BAs. Our current findings indicate that postbiotics alleviate ALD by activating FXR. Particularly, our analysis identified specific endogenous bile acids associated with FXR activation by postbiotics, such as 23-deoxycholic acid ($p < 0.05$), deoxycholic acid, lithocholic acid, and cholic acid. These results underscore the potential role of endogenous BAs in mediating the anti-ALD effects of postbiotics. Further research employing advanced strategies, such as small molecule accurate recognition technology (SMART)[54] is needed to uncover the functional components of postbiotics from natural sources and enhance our understanding of their mechanisms of action.

In conclusion, our findings reveal that postbiotics effectively mitigate ethanol-induced damage, encompassing hepatic steatosis, by modulating the FXR/SHP/SREBP-1c axis, both in vivo and in vitro. It is important to acknowledge certain limitations within our study, notably the challenge in identifying the specific active constituents of postbiotics. Nevertheless, this study contributes novel observations that enhance our understanding of the mechanistic underpinnings behind the protective effects of postbiotics in ethanol-induced liver injury.

Supporting Information

Supporting Information is available from the Wiley Online Library or from the author.

Acknowledgements

The authors thank the academician workstation of Southwest Medical University Hospital and academician (Expert) Workstation of Sichuan Province, Metabolic Hepatobiliary and Pancreatic Diseases Key Laboratory of Luzhou City for providing the experimental platform. They thank Shanghai Bioprofile Technology Co., Ltd. for technical support in bile acid (BA) quantification and detection of the functional metabolites in postbiotics.

This study was supported by grants from the National Natural Science Foundation of China (82170587), Natural Science Foundation of Sichuan Province (2022NSFSC1321; 2023YFS0144), Sichuan Science and Technol-

ogy Program (2022YFS0617 and 2022YFS0626), Southwest Medical University applied basic research project (2021ZKMS025), Luzhou Municipal Government–Southwest Medical University Cooperation Application Foundation (2021LZXNYD-J01), Luzhou Municipal People's Government-Southwest Medical University Science and Technology Strategic Cooperation Project (2021LZXNYD-Z01).

Conflict of Interest

The authors declare no conflict of interest.

Author Contributions

C.L.: formal analysis, methodology, writing – original draft, contribution to part of the experiments; T.C.: formal analysis, contribution to part of the experiments; Y.C.: contribution to part of the experiments; J.B.: contribution to part of the experiments. M.L.: contribution to part of the experiments; B.G.: contribution to part of the experiments; M.H.: supervision, writing–review and editing, conceptualization, funding acquisition; W.F.: supervision, writing–review and editing, funding acquisition, project administration.

Data Availability Statement

All data generated of analyzed during the current study are included in this published article or are available from the corresponding author.

Keywords

alcohol-associated liver diseases, FXR, *Lactobacillus reuteri*, lipid metabolism, postbiotics

Received: December 31, 2023
Revised: April 30, 2024
Published online:

[1] M. Thursz, A. Lingford-Hughes, *BMJ* **2023**, *383*, e077090.
[2] A. Louvet, P. Mathurin, *Nat. Rev. Gastroenterol. Hepatol.* **2015**, *12*, 231.
[3] C. L. Hsu, B. Schnabl, *Nat. Rev. Microbiol.* **2023**, *21*, 719.
[4] A. K. Singal, P. Mathurin, *JAMA, J. Am. Med. Assoc.* **2021**, *326*, 165.
[5] H. K. Seitz, R. Bataller, H. Cortez-Pinto, B. Gao, A. Gual, C. Lackner, P. Mathurin, S. Mueller, G. Szabo, H. Tsukamoto, *Nat. Rev. Dis. Primer* **2018**, *4*, 16.
[6] Y. Cheng, X. Xiang, C. Liu, T. Cai, T. Li, Y. Chen, J. Bai, H. Shi, T. Zheng, M. Huang, W. Fu, *J. Agric. Food Chem.* **2022**, *70*, 12550.
[7] T.-X. Zheng, S.-L. Pu, P. Tan, Y.-C. Du, B.-L. Qian, H. Chen, W.-G. Fu, M.-Z. Huang, *Front. Physiol.* **2020**, *11*, 595382.
[8] S. Zoghi, A. Abbasi, F. S. Heravi, M. H. Somi, Z. Nikniaz, S. Y. Moaddab, H. Ebrahimzadeh Leylabadlo, *Crit. Rev. Food Sci. Nutr.* **2024**, *64*, 2176.
[9] S. Salminen, M. C. Collado, A. Endo, C. Hill, S. Lebeer, E. M. M. Quigley, M. E. Sanders, R. Shamir, J. R. Swann, H. Szajewska, G. Vinderola, *Nat. Rev. Gastroenterol. Hepatol.* **2021**, *18*, 649.
[10] T. Teame, A. Wang, M. Xie, Z. Zhang, Y. Yang, Q. Ding, C. Gao, R. E. Olsen, C. Ran, Z. Zhou, *Front. Nutr.* **2020**, *7*, 570344.
[11] G. Vinderola, M. E. Sanders, S. Salminen, *Foods Basel Switz.* **2022**, *11*, 1077.
[12] S. Sabahi, A. Homayouni Rad, L. Aghebati-Maleki, N. Sangtarash, M. A. Ozma, A. Karimi, H. Hosseini, A. Abbasi, *Crit. Rev. Food Sci. Nutr.* **2022**, *63*, 8375.
[13] L. Sun, J. Cai, F. J. Gonzalez, *Nat. Rev. Gastroenterol. Hepatol.* **2021**, *18*, 335.
[14] Y.-D. Wang, W.-D. Chen, D. D. Moore, W. Huang, *Cell Res.* **2008**, *18*, 1087.
[15] X. Li, W. Lu, A. Kharitonenkov, Y. Luo, *J. Intern. Med.* **2024**, *295*, 292.
[16] M. Jiang, F. Li, Y. Liu, Z. Gu, L. Zhang, J. Lee, L. He, V. Vatsalya, H.-G. Zhang, Z. Deng, X. Zhang, S.-Y. Chen, G. L. Guo, S. Barve, C. J. McClain, W. Feng, *Hepatol. Baltim. Md.* **2022**, *77*, 1164.
[17] Y. Li, Y. Tian, W. Cai, Q. Wang, Y. Chang, Y. Sun, P. Dong, J. Wang, *J. Agric. Food Chem.* **2021**, *69*, 9813.
[18] B. L. Clifford, L. R. Sedgeman, K. J. Williams, P. Morand, A. Cheng, K. E. Jarrett, A. P. Chan, M. C. Brearley-Sholto, A. Wahlström, J. W. Ashby, W. Barshop, J. Wohlschlegel, A. C. Calkin, Y. Liu, A. Thorell, P. J. Meikle, B. G. Drew, J. J. Mack, H.-U. Marschall, E. J. Tarling, P. A. Edwards, T. Q. de Aguiar Vallim, *Cell Metab.* **2021**, *33*, 1671.e4.
[19] J. A. Linares-Pastén, R. Sabet-Azad, L. Pessina, R. R. R. Sardari, M. H. A. Ibrahim, R. Hatti-Kaul, *Bioresour. Technol.* **2015**, *180*, 172.
[20] S. Kim, J. Chen, T. Cheng, A. Gindulyte, J. He, S. He, Q. Li, B. A. Shoemaker, P. A. Thiessen, B. Yu, L. Zaslavsky, J. Zhang, E. E. Bolton, *Nucleic Acids Res.* **2021**, *49*, D1388.
[21] A. Daina, O. Michielin, V. Zoete, *Nucleic Acids Res.* **2019**, *47*, W357.
[22] M. Shklar, L. Strichman-Almashanu, O. Shmueli, M. Shmoish, M. Safran, D. Lancet, *Nucleic Acids Res.* **2005**, *33*, D556.
[23] J. Piñero, J. M. Ramírez-Anguita, J. Saüch-Pitarch, F. Ronzano, E. Centeno, F. Sanz, L. I. Furlong, *Nucleic Acids Res.* **2020**, *48*, D845.
[24] D. Szklarczyk, A. L. Gable, K. C. Nastou, D. Lyon, R. Kirsch, S. Pyysalo, N. T. Doncheva, M. Legeay, T. Fang, P. Bork, L. J. Jensen, C. von Mering, *Nucleic Acids Res.* **2021**, *49*, D605.
[25] D. W. Huang, B. T. Sherman, R. A. Lempicki, *Nat. Protoc.* **2009**, *4*, 44.
[26] Z. Pan, B. Mao, Q. Zhang, X. Tang, B. Yang, J. Zhao, S. Cui, H. Zhang, *Int. J. Mol. Sci.* **2022**, *23*, 13522.
[27] A. Bertola, S. Mathews, S. H. Ki, H. Wang, B. Gao, *Nat. Protoc.* **2013**, *8*, 627.
[28] P. Bhargava, M. D. Smith, L. Mische, E. Harrington, K. C. Fitzgerald, K. Martin, S. Kim, A. A. Reyes, J. Gonzalez-Cardona, C. Volsko, A. Tripathi, S. Singh, K. Varanasi, H.-N. Lord, K. Meyers, M. Taylor, M. Gharagozloo, E. S. Sotirchos, B. Nourbakhsh, R. Dutta, E. M. Mowry, E. Waubant, P. A. Calabresi, *J. Clin. Invest.* **2020**, *130*, 3467.
[29] T. Yang, T. Shu, G. Liu, H. Mei, X. Zhu, X. Huang, L. Zhang, Z. Jiang, *J. Steroid Biochem. Mol. Biol.* **2017**, *172*, 69.
[30] F. Zheng, X. Zhao, Z. Zeng, L. Wang, W. Lv, Q. Wang, G. Xu, *Nat. Protoc.* **2020**, *15*, 2519.
[31] F. Higuera-de la Tijera, A. I. Servín-Caamaño, A. E. Serralde-Zúñiga, J. Cruz-Herrera, E. Pérez-Torres, J. M. Abdo-Francis, F. Salas-Gordillo, J. L. Pérez-Hernández, *World J. Gastroenterol.* **2015**, *21*, 4975.
[32] A. Perino, H. Demagny, L. Velazquez-Villegas, K. Schoonjans, *Physiol. Rev.* **2021**, *101*, 683.
[33] P. Hartmann, K. Hochrath, A. Horvath, P. Chen, C. T. Seebauer, C. Llorente, L. Wang, Y. Alnouti, D. E. Fouts, P. Stärkel, R. Loomba, S. Coulter, C. Liddle, R. T. Yu, L. Ling, S. J. Rossi, A. M. DePaoli, M. Downes, R. M. Evans, D. A. Brenner, B. Schnabl, *Hepatol. Baltim. Md.* **2018**, *67*, 2150.
[34] I. Mohanty, C. Allaband, H. Mannochio-Russo, Y. El Abiead, L. R. Hagey, R. Knight, P. C. Dorrestein, *Nat. Rev. Gastroenterol. Hepatol.* **2024**, *21*, 493.
[35] M. H. Sarafian, M. R. Lewis, A. Pechlivanis, S. Ralphs, M. J. W. McPhail, V. C. Patel, M.-E. Dumas, E. Holmes, J. K. Nicholson, *Anal. Chem.* **2015**, *87*, 9662.
[36] H. Chu, L. Jiang, B. Gao, N. Gautam, J. A. Alamoudi, S. Lang, Y. Wang, Y. Duan, Y. Alnouti, E. E. Cable, B. Schnabl, *Transl. Res. J. Lab. Clin. Med.* **2021**, *227*, 1.
[37] M. You, G. E. Arteel, *J. Hepatol.* **2019**, *70*, 237.
[38] M. Watanabe, S. M. Houten, L. Wang, A. Moschetta, D. J. Mangelsdorf, R. A. Heyman, D. D. Moore, J. Auwerx, *J. Clin. Invest.* **2004**, *113*, 1408.

[39] Y. Fang, L. Hegazy, B. N. Finck, B. Elgendy, *J. Med. Chem.* **2021**, *64*, 17545.
[40] C. Li, W. Zhou, M. Li, X. Shu, L. Zhang, G. Ji, *Biomed. Pharmacother.* **2021**, *139*, 111587.
[41] S. Jeon, R. Carr, *J. Lipid Res.* **2020**, *61*, 470.
[42] Q. Liu, L. Xu, M. Wu, Y. Zhou, J. Yang, C. Huang, T. Xu, J. Li, L. Zhang, *Cell Biosci.* **2021**, *11*, 129.
[43] R. Sharma, M. Jadhav, N. Choudhary, A. Kumar, A. Rauf, R. Gundamaraju, A. F. AlAsmari, N. Ali, R. K. Singla, R. Sharma, B. Shen, *Front. Nutr.* **2022**, *9*, 1063118.
[44] T. Xia, B. Fang, C. Kang, Y. Zhao, X. Qiang, X. Zhang, Y. Wang, T. Zhong, J. Xiao, M. Wang, *Oxid. Med. Cell. Longev.* **2022**, *2022*, 5025237.
[45] A. Kumari, D. Pal Pathak, S. Asthana, *Int. J. Biol. Sci.* **2020**, *16*, 2308.
[46] B. Kong, M. Zhang, M. Huang, D. Rizzolo, L. E. Armstrong, J. D. Schumacher, M. D. Chow, Y.-H. Lee, G. L. Guo, *Dig. Liver Dis. Off. J. Ital. Soc. Gastroenterol. Ital. Assoc. Study Liver* **2019**, *51*, 570.
[47] B. Goodwin, S. A. Jones, R. R. Price, M. A. Watson, D. D. McKee, L. B. Moore, C. Galardi, J. G. Wilson, M. C. Lewis, M. E. Roth, P. R. Maloney, T. M. Willson, S. A. Kliewer, *Mol. Cell* **2000**, *6*, 517.
[48] F. Huang, X. Zheng, X. Ma, R. Jiang, W. Zhou, S. Zhou, Y. Zhang, S. Lei, S. Wang, J. Kuang, X. Han, M. Wei, Y. You, M. Li, Y. Li, D. Liang, J. Liu, T. Chen, C. Yan, R. Wei, C. Rajani, C. Shen, G. Xie, Z. Bian, H. Li, A. Zhao, W. Jia, *Nat. Commun.* **2019**, *10*, 4971.
[49] M. Sorribas, M. O. Jakob, B. Yilmaz, H. Li, D. Stutz, Y. Noser, A. de Gottardi, S. Moghadamrad, M. Hassan, A. Albillos, R. Francés, O. Juanola, I. Spadoni, M. Rescigno, R. Wiest, *J. Hepatol.* **2019**, *71*, 1126.
[50] R. M. Gadaleta, K. J. van Erpecum, B. Oldenburg, E. C. L. Willemsen, W. Renooij, S. Murzilli, L. W. J. Klomp, P. D. Siersema, M. E. I. Schipper, S. Danese, G. Penna, G. Laverny, L. Adorini, A. Moschetta, S. W. C. van Mil, *Gut* **2011**, *60*, 463.
[51] K. H. Kim, S. Choi, Y. Zhou, E. Y. Kim, J. M. Lee, P. K. Saha, S. Anakk, D. D. Moore, *Hepatol. Baltim. Md.* **2017**, *66*, 498.
[52] Y. Matsuda, N. Ozawa, T. Shinozaki, K.-I. Wakabayashi, K. Suzuki, Y. Kawano, I. Ohtsu, Y. Tatebayashi, *Transl. Psychiatry* **2020**, *10*, 170.
[53] L. Pernomian, M. Duarte-Silva, C. R. de Barros Cardoso, *Clin. Rev. Allergy Immunol.* **2020**, *59*, 382.
[54] C. Zhang, Y. Idelbayev, N. Roberts, Y. Tao, Y. Nannapaneni, B. M. Duggan, J. Min, E. C. Lin, E. C. Gerwick, G. W. Cottrell, W. H. Gerwick, *Sci. Rep.* **2017**, *7*, 14243.